JOURNAL OF MATERIALS SCIENCE 31 (1996) 1481–1487

Sintering of mullite-based particulate composites containing ZrO_2

NAGESWAR KAPURI*, K. N. RAI*‡, G. S. UPADHYAYA‡
Materials Science Programme and ‡Department of Materials and Metallurgical Engineering, Indian Institute of Technology, Kanpur 208016, India

ZrO_2 and its modified versions containing MgO and Y_2O_3 were selected as particulate reinforcement in order to achieve better mechanical properties of mullite. Particulate composites up to 25 vol % ZrO_2 and its modifications were pressed to 55% relative density at 300 MPa followed by sintering at 1600 °C and 1650 °C for one hour. Studies were conducted on fracture toughness, transverse rupture strength, hardness, dielectric constant, microstructure and fractography. Composites sintered at 1650 °C were found superior in properties than those at 1600 °C. The maximum strength of mullite composites was observed at a composition of 10 vol % ZrO_2.

1. Introduction

Mullite ceramics are extensively used in different structural applications, as the elongated needle-shaped crystals give it good mechanical properties. However, it possesses low fracture toughness due to its intrinsic brittleness [1]. Further improvement in mechanical properties can be achieved by incorporating ZrO_2 particules in the mullite matrix, which can be done in the precursor materials by the reaction sintering [2–8] method. The sol–gel method [1] is also important for the preparation of homogeneously distributed composites. However, this is relatively expensive and mainly limited to research.

For the commercial production of composites based on mullite, ZrO_2 is a very useful additive. These are prepared by milling/compaction and sintering of the premixed powders [9]. Premullite powders [10] have also been used for such composites. Mullite–ZrO_2 glass powders [11] were also tried, but a lower density of finished products limits their use in actual applications. In the present investigation an attempt has been made to prepare mullite–ZrO_2 and modified mullite–ZrO_2 composites by the milling/sintering route.

2. Experimental procedure

The characteristics of different powders used in the present investigation are given in Table I. Mullite powders with 0–25 vol % ZrO_2 were mixed by the conventional ball-milling technique. Wet milling of the powders was performed in isopropyl alcohol medium for a period of 3 h. The ratio of powder to balls by mass was kept at 1 : 3. The wet mixed powders were dried at 110 °C. From the ball-milled powder, rectangular compacts measuring 25 mm × 8 mm × 2.6 mm were prepared at a pressure of 300 MPa to a green density of approximately 55% of theoretical using PVA as a binder.

Sintering of the green compacts was carried out in a super Kanthal resistance heated furnace at 1600 °C and 1650 °C, respectively, for 1 h in normal atmosphere. The former temperature was selected only for ZrO_2 additive, but the latter was used for all additives. The heating rate was 5 °C min^{-1}. During heating the temperature was held at 450 °C for 15 min to make sure that no sample damage occurred during binder removal.

The sintered densities were measured with the help of a Fairey Tecramics Ltd (UK) Mercury Densometer using the following formula:

$$\text{Sintered density (g cm}^{-3}) = \frac{W_1 \times d}{W_2}$$

where

W_1 = weight of sample in air (g)
W_2 = weight of sample in mercury (g)
d = density of mercury (g cm^{-3})

Sintered porosity was calculated using the values of sintered and theoretical densities. The latter was calculated using the rule of mixture, which assumes no chemical interaction between the components.

The transverse rupture strength (TRS) of the as-sintered samples was measured under a three-point bending load in an Instron machine with a crosshead speed of 0.2 mm min^{-1}. The load at the point of failure of the test piece was used in the following formula for calculating the TRS:

$$\text{TRS (MPa)} = \frac{1.5\,PL}{WD^2} \times 9.806$$

where

P = breaking load (kg)
L = span length (mm)
W = width (mm)
D = thickness (mm)

0022–2461

TABLE I Characteristics of different ceramic powders

(a) *Mullite powder*
Supplier: Chichibu Cement Co. Ltd, Japan
Average particle size = 1.3 μm
Specific surface area = 10 $m^2 g^{-1}$
Al_2O_3 : SiO_2 = 1.5
Apparent density = 0.59 g cm^{-3}

(b) *ZrO_2 powder*
Supplier: Magnesium Elektron Ltd, UK
Chemical composition (mass %): SiO_2 0.15, TiO_2 0.20, Fe_2O_3 0.02
Average particle size = 1.1 μm
Specific surface area = 3.0 $m^2 g^{-1}$
Apparent density = 1.06 g cm^{-3}

(c) *ZrO_2–MgO powder*
Supplier: Dynamit Nobel, Germany
Chemical composition (mass %): SiO_2 0.06, TiO_2 < 0.05, Fe_2O_3 0.04, CaO 0.04, MgO 3.41, Al_2O_3 0.05, HfO_2 1.69, Na_2O 0.01, K_2O < 0.01, ZrO_2 94.7
Average particle size = 50% < 0.6 μm
Specific surface area = 15 $m^2 g^{-1}$
Apparent density = 0.45 g cm^{-3}

(d) *ZrO_2–MgO–Y_2O_3 powder*
Supplier: Dynamit Nobel, Germany
Chemical composition (mass %): SiO_2 0.05, TiO_2 < 0.05, Fe_2O_3 0.04, CaO 0.04, MgO 2.50, Al_2O_3 0.06, HfO_2 1.60, Na_2O 0.01, K_2O < 0.01, Y_2O_3 3.7, ZrO_2 92.0
Average particle size = 50% < 0.6 μm
Specific Surface Area = 21 $m^2 g^{-1}$
Apparent Density = 0.38 g cm^{-3}

For each set of preparations, six specimens were tested and the average value was reported.

The three-point bending fracture toughness (K_{IC}) was measured according to the method described by Larson *et al.* [12]. In this method a very fine notch was cut at the middle of the as-sintered sample with the help of a diamond cutter. A three-point bending load was also used here to find the load at the point of failure. The formula [12] used for the measurement was:

$$K_{IC} = \frac{3PLC^{1/2}}{2WD^2}\left[A_0 + A_1\left(\frac{C}{D}\right) + A_2\left(\frac{C}{D}\right)^2 + A_3\left(\frac{C}{D}\right)^3 + A_4\left(\frac{C}{D}\right)^4\right] \times (1000)^{-1/2} \text{ MPa m}^{1/2}$$

where

P = breaking load (N)
L = span (mm)
D = thickness (mm)
W = width (mm)
C = notch length (mm, generally $c \simeq D/2$)
$A_0 = 1.90 + 0.0075L/D$
$A_1 = -3.39 + 0.08L/D$
$A_2 = 15.4 - 0.2175L/D$
$A_3 = -26.24 + 0.2815L/D$
$A_4 = 26.38 - 0.145L/D$

In this case also the load was applied in an Instron machine, the crosshead speed of which was set at 0.05 mm min^{-1}. Three test samples were broken for each set and the average value was reported.

The hardness of the sintered and polished compacts was measured on a Vickers hardness testing machine Model HPO 250 (Fritz Heckert, Leipzig) using a load of 196 N. The average value of four tests was reported.

Microstructure and fractography studies were carried out in a Jeol 840A scanning electron microscope. Polished samples etched in 10% HF were used for this purpose. To make the surface conductive to the electron beam, samples were vacuum-coated with silver. Secondary electrons were used in the mode of operation at an operating voltage of 15 kV.

The X-ray diffractometric method was used for calculating the fractional tetragonal and monoclinic zirconia present in the sintered samples. A Rich. Seifert and Co. (Germany) model III diffractometer was used at a scanning rate of 1.2° min^{-1} (2θ) and a time constant of 10 s along with CuK_α radiation.

Dielectric constants were measured in a Hewlett Packard 4194A Impedance/Gain-phase Analyser, using polished and silver-coated rectangular specimens. Dielectric constants (K) were measured at 1 MHz frequency using the following formula:

$$K = 1 + \frac{C_p - C_o}{\varepsilon_o A} t$$

where

C_p = capacitance of specimen (F)
C_0 = capacitance of air (F)
t = thickness (m)
A = area (m^2)
ε_0 = permittivity of free space (8.85 × 10^{12} F m^{-1})

3. Results

3.1. Sintered density and total porosity

The sintered density and % total porosity variations of mullite–ZrO_2 composites, sintered at 1600 °C, are shown in Fig. 1. It is clear that sintered density increases with increase in vol % ZrO_2 added. This is as expected, since ZrO_2 has a higher density than mullite. However, the % total porosity decreases to an optimum value, then remains constant with increase in ZrO_2, except at 25 vol % ZrO_2 where it again increases slightly. Fig. 2 shows the variation in sintered density of mullite-based composites, when sintered at 1650 °C. The maximum scatter in the values was 5.2%. From the figure it is apparent that the same general trend is observed for the increase in density values with increase in ZrO_2 additive as for 1600 °C sintering. However, such a trend is absent in the case of modified ZrO_2 addition. Fig. 3 shows that sintered porosity variation does not have any regular trend with respect to vol % of additive. However, in the case of MgO–Y_2O_3 modified ZrO_2 addition, there is some indication of a rise in sinterability at 10 vol %.

3.2. Mechanical properties

Transverse rupture strength (TRS) variation of mullite–ZrO_2 composites sintered at 1600 °C is shown in Fig. 4, from which it is evident that TRS passes through a maximum at 10 vol % ZrO_2. The values for

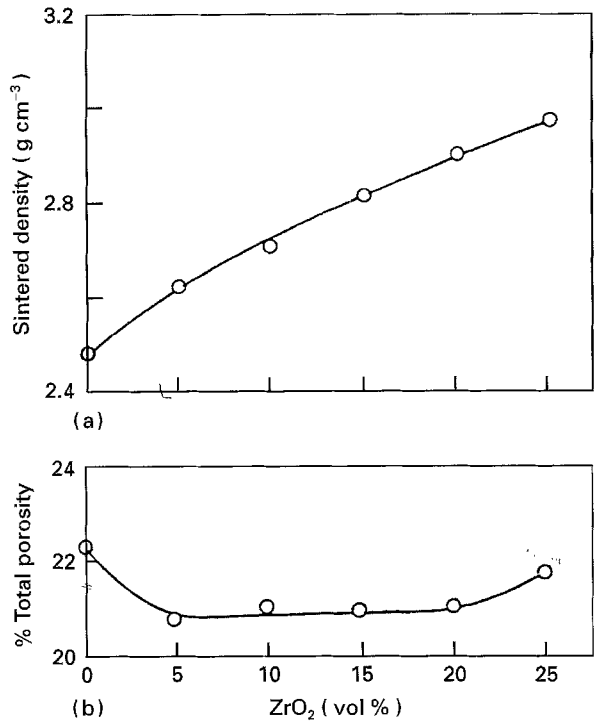

Figure 1 Variation of sintered density and % total porosity of mullite-ZrO_2 composites, sintered at 1600°C.

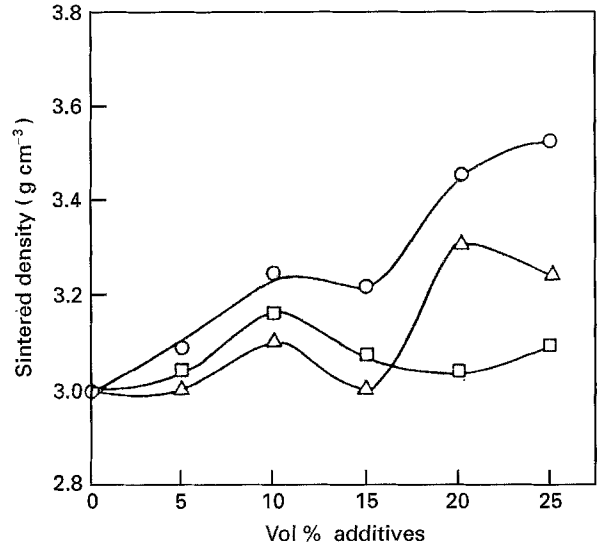

Figure 2 Variation of sintered density of mullite-based composites, sintered at 1650°C. (○) Mullite–ZrO_2, (△) mullite–ZrO_2–MgO, (□) mullite–ZrO_2–MgO–Y_2O_3.

composites sintered at 1650°C are higher (Fig. 5) than the composites sintered at 1600 °C. The trend in the plots is the same for both sintering temperatures. The maximum scatter in the data was 39%.

Fracture toughness (K_{IC}) variation of mullite-based composites sintered at 1650 °C is shown in Fig. 6. Unlike TRS variation, the K_{IC} does not change with any specific trend. However, one thing is encouraging: the values for most of the composites are higher than for straight mullite. The maximum variation in the toughness values was 20%.

The Vickers hardness variation of mullite–ZrO_2 composites sintered at 1600 °C (Fig. 7) shows that the

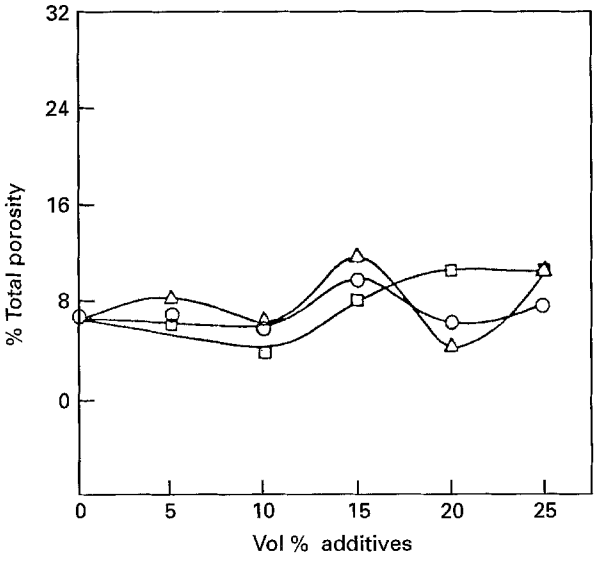

Figure 3 Variation of % total porosity of mullite-based composites, sintered at 1650°C. (○) Mullite–ZrO_2, (△) mullite–ZrO_2–MgO, (□) mullite–ZrO_2–MgO–Y_2O_3.

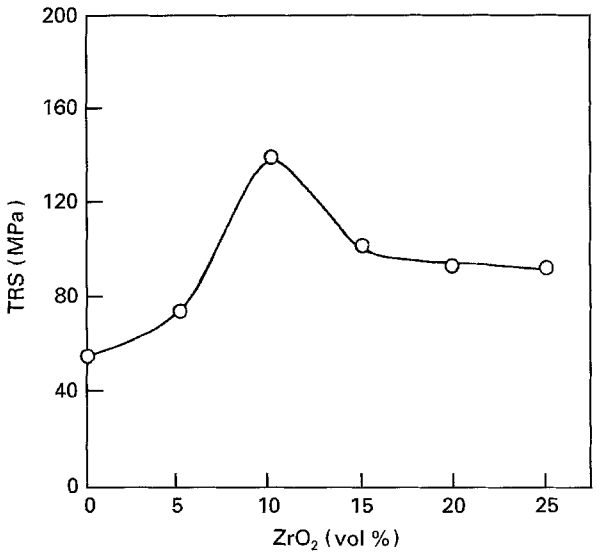

Figure 4 Variation of transverse rupture strength of mullite–ZrO_2 composites, sintered at 1600°C.

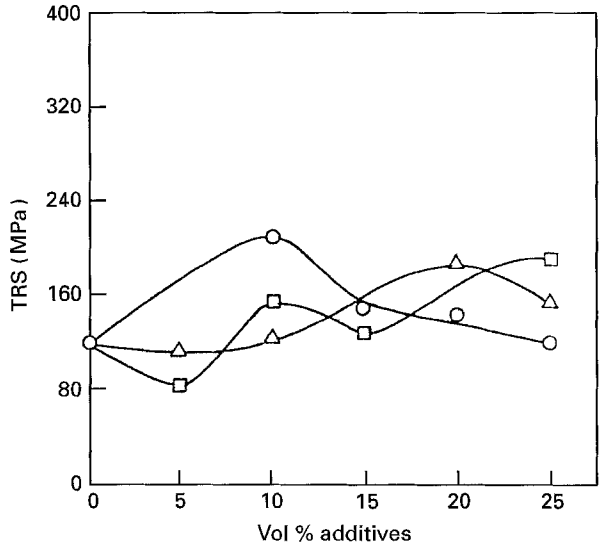

Figure 5 Variation of transverse rupture strength of mullite-based composites, sintered at 1650°C. (○) Mullite–ZrO_2, (△) mullite–ZrO_2–MgO, (□) mullite–ZrO_2–MgO–Y_2O_3.

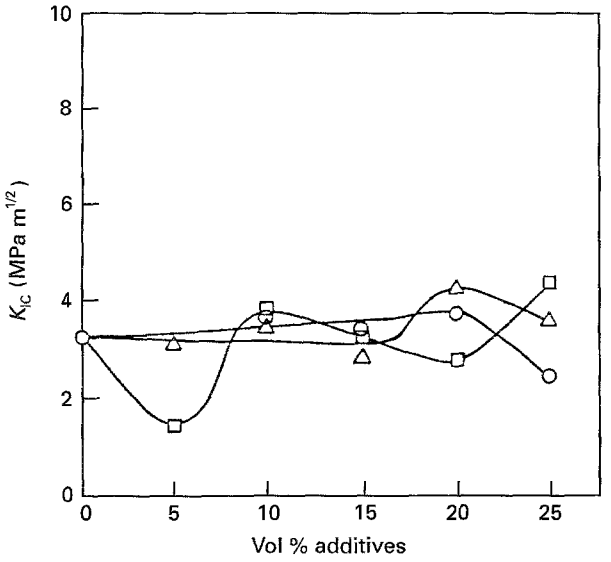

Figure 6 Variation of fracture toughness of mullite-based composites, sintered at 1650°C. (○) Mullite–ZrO_2, (△) mullite–ZrO_2–MgO, (□) mullite–ZrO_2–MgO–Y_2O_3.

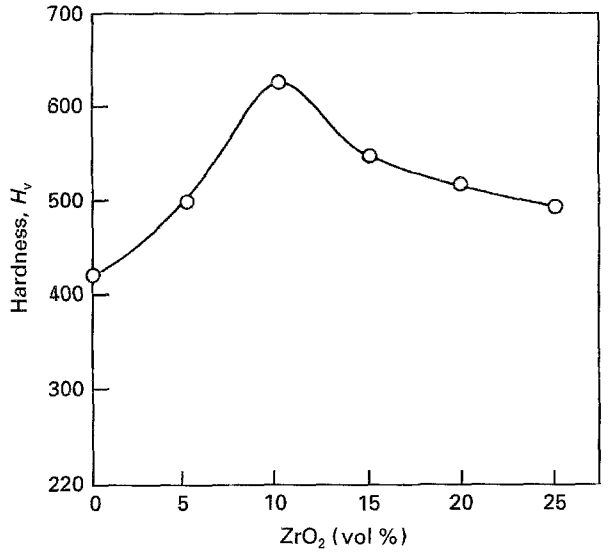

Figure 7 Variation of Vickers hardness for mullite–ZrO_2 composites, sintered at 1650°C.

value in general increases with increase in vol % ZrO_2, with a peak at an optimum composition of 10 vol % ZrO_2.

3.3. SEM fractography, microstructure and EDX analysis

From the fractographic analysis (Fig. 8) it is clear that the fracture mode is intergranular. In some cases dimple formation also occurs. The second phase, mainly ZrO_2, distributes itself uniformly in the slightly elongated matrix. The ZrO_2 is almost rounded in morphology and its size increases in the range of 0.45–2.2 μm, with increase in its content in the composites.

Fig. 9 shows the SEM microstructures and EDX spot mappings of zirconium for the composites sintered at 1650 °C. The microstructure shows a mixture of a chunky as well as a needle-shaped matrix. The

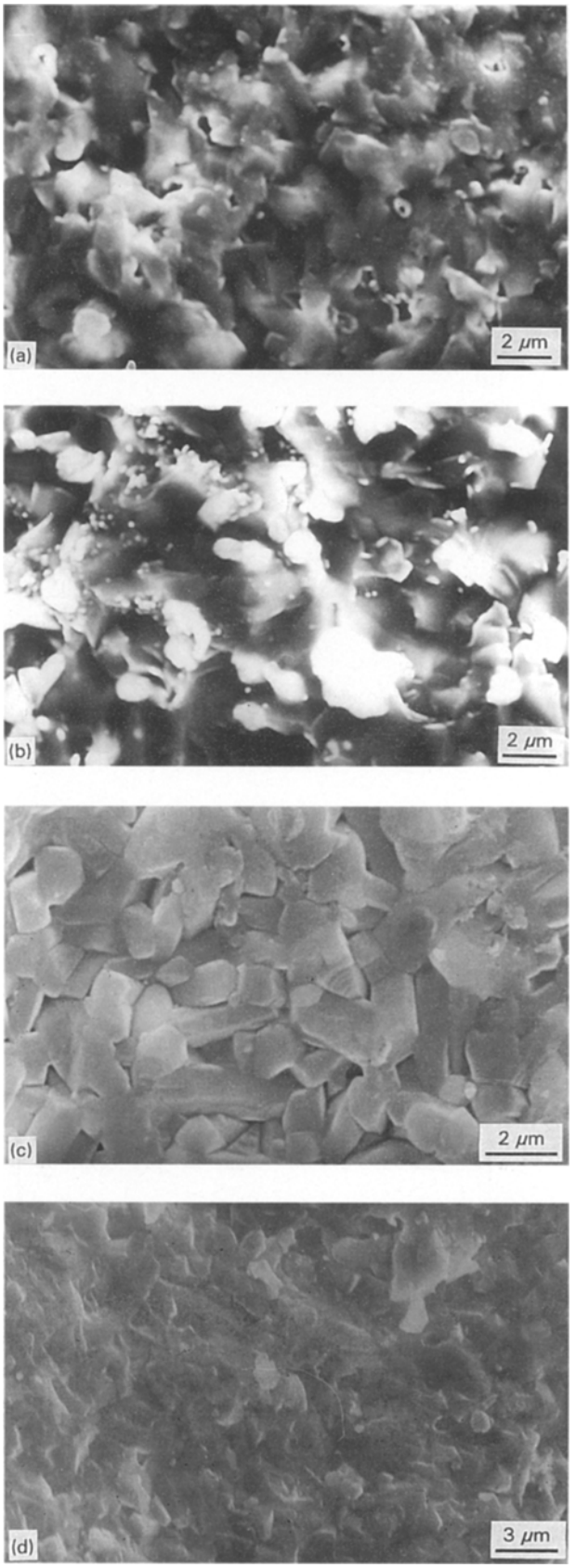

Figure 8 Fractographs of mullite-based composites, sintered at 1650°C. (a) 0 vol % additive, (b) 10 vol % ZrO_2, (c) 10 vol % ZrO_2–MgO, (d) 10 vol % ZrO_2–MgO–Y_2O_3.

ZrO_2 particles are almost rounded and distributed homogeneously throughout the matrix. From the spot mappings of zirconium a uniform distribution of ZrO_2 throughout the matrix irrespective of the composite composition is noticed.

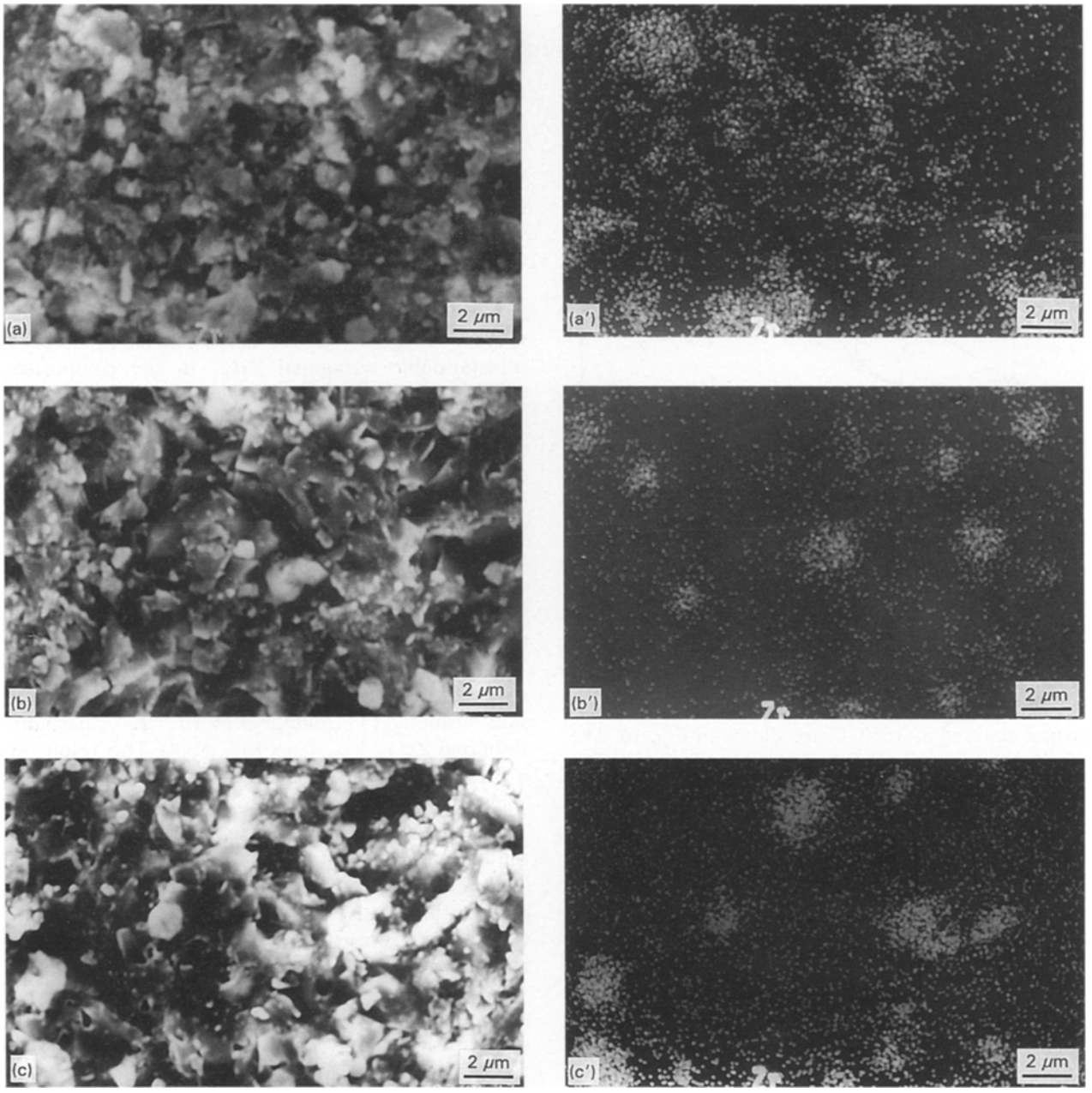

Figure 9 SEM microstructures (left) and EDX spot mappings of Zirconium (right) for mullite-based composites, sintered at 1650°C. (a) 0 vol % ZrO_2, (b) 10 vol % ZrO_2–MgO, (c) 10 vol % ZrO_2–MgO–Y_2O_3.

TABLE II Fraction of monoclinic (f_m) and tetragonal–ZrO_2 (f_t) present in mullite-based composites, sintered at 1650 °C for 1 hour

Additive (vol %)	Mullite–ZrO_2		Mullite–ZrO_2–MgO		Mullite–ZrO_2–MgO–Y_2O_3	
	f_t	f_m	f_t	f_m	f_t	f_m
5	0.39	0.61	0.66	0.34	0.68	0.32
10	0.33	0.67	0.48	0.52	0.88	0.12
15	0.21	0.79	0.33	0.67	0.64	0.36
20	0.10	0.90	0.44	0.56	0.35	0.65
25	0.11	0.89	0.62	0.38	0.68	0.32

3.4. X-ray analysis

Table II shows the fractional amount of tetragonal and monoclinic phases of ZrO_2 in the composites, sintered at 1650 °C, obtained from XRD. It is obvious that for any fixed vol % of the composites, the volume fraction of tetragonal zirconia increases progressively while passing from straight composite to MgO and MgO/Y_2O_3 modified ZrO_2-containing composites. However, there is an exception in case of 20 vol % ZrO_2-containing composites. The X-ray diffraction results did not reveal any detectable presence of cubic ZrO_2 in any of the composites investigated.

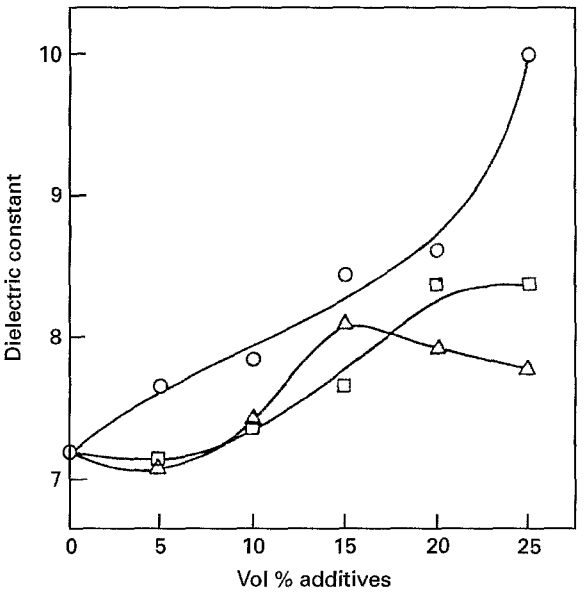

Figure 10 Variation of dielectric constant of mullite-based composites, sintered at 1650°C. (○) Mullite–ZrO_2, (△) mullite–ZrO_2–MgO, (□) mullite–ZrO_2–MgO–Y_2O_3.

3.5. Dielectric constant

Dielectric constant variations of mullite-based composites sintered at 1650 °C are shown in Fig. 10. The maximum scatter in the data was less than 1%. The dielectric constant increased with increase in the amount of additive. In the case of mullite–ZrO_2–MgO composite, however, it decreased slightly above 15 vol % additions. However, the increase is higher for mullite–ZrO_2 composites than for the other composites.

4. Discussion

Densification of mullite–ZrO_2 composites mainly occurs through solid-state sintering mechanisms, where the surface free energy is lowered with the associated elimination of solid–vapour interfaces. However, in the present study, the formation of a small amount of liquid phase during sintering due to the presence of impurities such as Na_2O, CaO, K_2O, Fe_2O_3, etc., cannot be ruled out [13]. The starting powders of ZrO_2 used in the present work contain 0.25–0.37% other oxides as impurities, and therefore the existence of a liquid phase during sintering is probable. The decrease in total sintered porosity with ZrO_2 addition (Fig. 1b), reveals the increasing sinterability of the composites. ZrO_2 additive retards the grain growth of mullite phase and promotes densification, which supports the findings of Prochazka *et al.* [14]. Higher amounts of additives, however, lead to coarsening of ZrO_2 particles. In addition, some shape change in the mullite matrix during sintering occurs as observed from the fractographs (Fig. 8). Both the above features may lead to poor sinterability of mullite. Local agglomeration of fine particles of both matrix and additives may also cause an adverse effect on the sintered properties of the composites. It is evident that at 10 vol % ZrO_2, a homogeneous microstructure gives rise to optimum densification (Fig. 9).

As is evident from Table II, both MgO and Y_2O_3 have a stabilizing effect on ZrO_2. For a fixed volume fraction of additive, the fractional amount of tetragonal phase increases in the order unmodified/MgO-modified/MgO–Y_2O_3-modified zirconia. This is the same as the established findings [15]. It is apparent that direct comparison of ZrO_2 (straight or modified) powders as far as their role on the properties of the composite is concerned is difficult, since their powder characteristics are not similar (Table I).

The increase in transverse rupture strength and fracture toughness with increase in vol % additives may be attributed to the associated stress-induced transformable tetragonal ZrO_2 in the composites [12], apart from the strengthening effect of the dispersoid. At a still higher vol % of additives, the particle size of ZrO_2 in the sintered composites increases, as evinced in the present investigation (Fig. 8). This is due to the increased chances of Ostwald ripening [16], because of the decreased ZrO_2–ZrO_2 interparticle spacing. Coarsening of ZrO_2 particles above a critical size, therefore, would lead to the spontaneous transformation of the tetragonal fraction to the monoclinic during postsintering cooling. The proportion of t-ZrO_2 is therefore reduced and at the same time extensive microcracking occurs due to the thermal expansion mismatch [1] (mullite: $5.7 \times 10^{-6}\ K^{-1}$; partially stabilized ZrO_2: $8.0–10.6 \times 10^{-6}\ K^{-1}$). This results in a fall in the strength of the composites. A decrease in Vickers hardness beyond the optimum composition of 10 vol % ZrO_2 (Fig. 7) is attributed to the decrease in the amount of t-ZrO_2 in the composites. The optimum TRS for different dispersoid composites at different compositions can be judged from the fact that the characteristics of the different powders are not identical.

As is well known in ceramic systems, microcracking has a beneficial effect on fracture toughness (K_{IC}), with the result that the K_{IC} of the composites continuously increases with increase in the vol % additives even beyond the optimum composition, where TRS is maximal. The existence of a solid solution far off the equilibrium at the mullite–ZrO_2 grain boundary [17] is not ruled out either, which would increase K_{IC} values. Since the solid solution region is assumed to be a dissipation energy region, it avoids crack propagation, thus leading to a higher toughness of the composites. The higher K_{IC} values for MgO-modified ZrO_2-containing composites compared with only ZrO_2-containing ones may be attributed to the cross-linked microstructure of mullite matrix [18]. This has been noticed to some extent in the present investigation (Fig. 8c).

Increase in dielectric constant (K) with increase in vol % additives in mullite is obviously due to the higher K values of the additive (ZrO_2: 12.00) than the mullite matrix (6.60). Due to the morphological differences in the starting powders, the increase in the dielectric constant for different composites is not comparable. The decrease in K values for mullite with greater than 15 vol % MgO-modified ZrO_2 additive may be due to the presence of an agglomeration of fine particles, leading to higher residual sintered porosities.

5. Conclusions

1. An optimum ZrO_2 addition enhances the sinterability of mullite–ZrO_2 composites prepared by the milling/sintering route.

2. For any fixed vol % dispersoid composite, the role of MgO or MgO/Y_2O_3 addition in ZrO_2 is to stabilize t-ZrO_2 in increasing order.

3. TRS variation shows a trend such that at a critical dispersoid addition the value is maximal. However, such a trend is not present in K_{IC} variation.

4. The dielectric constant increases with the increase in vol % of straight or modified ZrO_2 in the mullite.

References

1. M. G. M. U. ISMAIL, Z. NAKAI and S. SOMIA, in "Advances in Ceramics", Vol. 24, "Science and Technology of Zirconia III" (The American Ceramic Society, Westerville, 1988) p. 119.
2. N. CLAUSSEN and J. JOHN, *J. Am. Ceram. Soc.* **63** (1980) 228.
3. P. BOCH and J. P. GIRY, *Mater. Sci. Engng* **71** (1985) 39.
4. C. B. DE-LA. LASTRA, C. LEBLUD, A. LERICHE, F. CHAMBIER and M. R. ANSEAU, *J. Mater. Sci. Lett.* **4** (1985) 1099.
5. P. BOCH and J. P. GIRY, in "High Tech Ceramics", edited by P. Vincenzini (Elsevier Science Publishers, Amsterdam, 1989) p. 851.
6. J. V. EMILIANO and A. M. SEGADAES, in "Zirconia 88: Advances in Zirconia Science and Technology", edited by S. Meriani and C. Palmonari (Elsevier Applied Science, Barking, 1988) p. 51.
7. M. HOLMSTROM, T. CHARTIER and P. BOCH, in "Ceramic Materials Research—I" edited by R. J. Brook (North Holland, Amsterdam, 1989) p. 105.
8. P. DESCAMPS S. SAKAGUCHI, M. POORTEMAN and F. CHAMBIER, *J. Am. Ceram. Soc.* **74** (1991) 2476.
9. YUAN QU-MING, TAN JIA-QI and JIN JHENG GUO, *J. Am. Ceram. Soc.* **69** (1986) 265.
10. J. S. MOYA and M. I. OSENDI, *J. Mater. Sci. Lett.* **2** (1983) 599.
11. R. MCPHERSON, *J. Am. Ceram. Soc.* **69** (1986) 297.
12. D. R. LARSON, J. A. COPPOLA and D. P. H. HASSELMAN, *J. Am. Ceram. Soc.* **57** (1974) 417.
13. R. F. DAVIS and J. A. PASK, Mullite, in "High Temperature Oxides", Part IV, edited by A. M. Alper (Academic Press, New York, 1971) p. 37.
14. S. PROCHAZKA, J. S. WALLACE and N. CLAUSSEN, Microstructure of Sintered Mullite-Zirconia Composites, *ibid.* **66** (1983) C-125.
15. D. J. GREEN, R. H. J. HANNINK and M. V. SWAIN, "Transformation Toughening of Ceramics" (CRC press, Boca Raton, Florida, 1989) p. 45.
16. J. S. WALLACE, N. CLAUSSEN, M. RÜHLE and G. PETZOW, in "Materials Science Research", Vol. 14, edited by J. A. Pask and A. G. Evans (Plenum, New York, 1981) p. 155.
17. M. I. OSENDI, P. MIRANZO and J. S. MOYA, *J. Mater. Sci. Lett.* **4** (1985) 1026.
18. A. LERICHE, in "Mullite and Mullite Matrix Composites, Ceramic Transactions", Vol. 6, edited S. Somiya, R. F. Davis and J. A. Pask (The American Ceramic Society, Westerville, 1990) p. 541.

Received 31 October 1994
and accepted 5 April 1995